Available online at www.sciencedirect.com
ScienceDirect
Ocean Engineering 35 (2008) 165–173
OCEAN ENGINEERING
www.elsevier.com/locate/oceaneng

Mooring forces in horizontal interlaced moored floating pipe breakwater with three layers

Arkal Vittal Hegde[a,*], Kiran Kamath[b], J.C. Deepak[a]

[a]Department of Applied Mechanics and Hydraulics, National Institute of Technology Karnataka, Surathkal, Srinivasnagar, Mangalore 575 025, India
[b]Department of Civil Engineering, MIT, Manipal, Karnataka 576 104, India

Received 26 November 2006; accepted 6 August 2007
Available online 11 August 2007

Abstract

The paper presents the results from model scale experiments on the study of forces in the moorings of horizontally interlaced, multi-layered, moored floating pipe breakwaters. The studies are conducted with breakwater models having three layers subjected to waves of steepness H_i/L (H_i is the incident wave height and L the wavelength) varying from 0.0066 to 0.0464, relative width W/L (W is the width of breakwater) varying from 0.4 to 2.65, and relative spacing S/D (S is the spacing of pipes and D the diameter of pipe) of 2 and 4. The variation of measured normalized mooring forces on the seaward side and leeward side are analyzed by plotting non-dimensional graphs depicting $f/\gamma W^2$ (f is the force in the mooring per unit length of the breakwater, γ the weight density of sea water) as a function W/L for various values of H_i/d (d is the depth of water). It is found that the force in the seaward side mooring increases with an increase in H_i/L for d/W values ranging between 0.081 and 0.276. The experimental results also reveal that the forces in the seaward side mooring decrease as W/L increases, up to a value of $W/L = 1.3$, and then increases with an increase in W/L. It is also observed that the wave attenuation characteristics of breakwater model with relative spacing of 4 is better than that of the model with relative spacing of 2. The maximum force in the seaward side mooring for model with $S/D = 4$ is lower compared to that for the breakwater model with $S/D = 2$. A multivariate non-linear regression analysis has been carried out for the data on mooring forces for the seaside and leeside.

Keywords: Floating pipe breakwater; Relative width; Mooring force; Relative spacing; Wave steepness; Relative wave height

1. Introduction

Invariably, floating breakwaters are conceived either based on the concept of reflecting the wave energy or dissipating wave energy by induced turbulent motion. In recent times, many different types of floating breakwater models have been tested and some have been prototype constructed and their performance assessed. The prime factor in the construction of the floating breakwaters is to make the width of the breakwater (in the direction of wave propagation) greater than one-half the wavelength but preferably as wide as the incident wavelength; else, the breakwater rides over the top of the wave without attenuating the incident wave energy. Further, to be effective, the floating breakwater must be moored in place with both leeward and windward ties; otherwise, it would sag off and ride over the incident wave. A large degree of attenuation of wave heights and less force in the moorings should be the condition to be achieved for optimum design.

The development of floating breakwaters by various investigators has been influenced by several important features; large mass, large moment of inertia, and the combinations of two or more of the concepts of large effective mass or moment of inertia. Most of the literature available indicates that the parameter ''relative width'' greatly influences the wave attenuation characteristics of the breakwater. The design of a floating breakwater is complicated and is an iterative process due to the interdependency of a number of associated design factors. For example, wave transmission performance depends on breakwater geometry, mass, and mooring properties. Similarly, mooring forces depend on breakwater geometry

*Corresponding author. Tel.: +91 824 2474050; fax: +91 824 2474033.
E-mail addresses: arkalvittal@gmail.com (A.V. Hegde), kiranmitin@yahoo.com (K. Kamath).

0029-8018/$ - see front matter © 2007 Elsevier Ltd. All rights reserved.
doi:10.1016/j.oceaneng.2007.08.001

Nomenclature

D	diameter of pipes
d	still water depth
f	force per unit length of breakwater
f_s	seaward side force per unit length of breakwater
f_l	leeward side force per unit length of breakwater
$f/\gamma W^2$	normalized mooring force
g	acceleration due to gravity
H_i	incident wave height
H_i/L	incident wave steepness
H_t	transmitted wave height
K_t	transmission coefficient
L	wavelength
n	number of layers of pipes
S	spacing between pipes
S/D	ratio of spacing to diameter of pipes
T	wave period
W	width of breakwater
W/L	relative breakwater width
γ	weight density of water
H_i/d	relative wave height

and mass. Finally, breakwater structural integrity depends on breakwater geometry, mass, and mooring forces. In the present state of art technology, neither an integrated nor an accepted methodology for the design of floating breakwaters is available. Instead, most designs have been prepared in an ad-hoc manner using one approach for evaluation of wave transmission, a separate approach for mooring force determination, and yet another approach for breakwater structural integrity.

Harris and Webber (1968) carried out a series of tests on floating breakwater models to measure wave attenuation and mooring forces. It was concluded that the mooring forces were at their maximum for wavelength/solid breadth ratio between 1.0 and 2.0, whereas, if the ratio is beyond 2.0, the forces diminished abruptly. Brebner and Ofuya (1968) conducted studies on an "A" frame and concluded that the peak mooring forces were about 1.5–2 times the average mooring forces.

Chen and Wiegel (1970) designed three rigid floating breakwaters and added two more later, each making use of a different mechanism or combination of mechanisms of wave energy dissipation and reflection. The tension in the mooring line consisted in general of two components, one caused by the rolling motion of the breakwater, and another caused by wave crests striking the structure. Harms (1979) presented design curves for the Goodyear floating tire breakwater based on the laboratory tests, and additionally substantiated by available full scale data. Two important floating tire breakwater design parameters have been assessed over a practical range of conditions, i.e. the breakwater size required for a desired level of wave attenuation and the associated peak mooring force. Arunachalam and Raman (1980) have presented a useful semi-empirical relation to evaluate the wave transmission and the peak mooring forces of a floating breakwater system.

Yamamoto et al. (1980) solved the problems of wave transformation and motions of elastically moored floating objects by direct use of Green's identity formula and validated their solutions with experimental investigations. They reported that the wave attenuation by a breakwater with small draft can be improved several times if the mooring system is properly arranged in comparison with same floating breakwater when it is conventionally moored. Based on large scale model tests on elastically moored floating breakwaters under the action of regular and random waves, Yamamoto (1981) reported that the response of elastically moored floating breakwater to random waves was essentially the same as the response of the breakwater to periodic waves.

Bishop (1982) made a comparative study of the design curves of Harms (1979) and the Coastal Engineering Research Center (CERC). The test results of Harms (1979) and CERC were in good agreement. Miller and Christensen (1984) predicted the dynamic response of floating breakwaters using a frequency domain analysis and compared it with full scale field measurements.

Based on experimental results of model tests on Y-frame floating breakwater Mani (1991) concluded that in order to achieve a transmission coefficient of less than 0.5, the relative width has to be around 0.15. The studies also revealed that for small values of wave parameter H_i/gT^2 (0.0025), the Y-frame floating breakwater predicted a 13.5% increase in the mooring force compared to twin pontoon floating breakwater and for H_i/gT^2 values between 0.0025 and 0.012, the Y-frame floating breakwater predicted an increase in mooring forces ranging between 50% and 100%. Isaacson and Wu (1995) investigated the response of a moored vessel to beam waves based on an idealized representation of the nonlinear stiffness characteristics of the mooring system.

Murali and Mani (1997) studied conventional floating breakwaters and the feasibility of developing a cage floating breakwater was explored. It was concluded that, though the stiffness of mooring lines does not modify the hydrodynamic performance characteristics of the breakwater, use of mooring lines with adequate stiffness is essential. Based on the experimental and theoretical investigations on the behavior of pontoon type floating breakwaters, Sannasiraj et al. (1998) concluded that theoretical and experimental measurements showed good agreement except at the roll resonance frequency. The

transmission coefficient was not significantly affected by the various mooring configurations studied. The mooring at the water surface and at the bottom of the floating breakwater yielded significantly smaller mooring forces than those obtained with crossed mooring.

Sundar et al. (2003) studied the hydrodynamic performance characteristics of a floating pipe breakwater (FPBW) model (row of pipes separated by a distance equivalent to the pipe diameter) moored to the flume floor with a slack mooring. Average reflection and transmission coefficients were evaluated as a function of relative breakwater width W/L. The mooring forces decreased with increase in W/L above 0.6. Hegde et al. (2007) studied the transmission characteristics of horizontal interlaced multilayer moored FPBW model with three layers of PVC pipes and relative spacing of 5.

The literature survey carried out clearly indicates that the studies on forces in the mooring lines of horizontal interlaced moored floating pipe breakwater (HIMMFPB) model has not been carried out. Hence, the scope of the present paper revolves around the study of forces in the seaward side and leeward side mooring lines of this type of breakwater (HIMMFPB) models in the regular wave flume of the department of Applied Mechanics and Hydraulics of National Institute of Technology Karnataka (NITK), Surathkal, Mangalore, Karnataka, India. The floating breakwater model is fabricated using universally available polyvinyl chloride (PVC) pipes, which are relatively inexpensive, and effortlessly available everywhere. These moored floating breakwaters may be used to create a temporary harbor area for small size boats, to create a tranquil area around an offshore structure, and to mitigate beach erosion during storm weather conditions. The breakwater model considered in the present study dissipates the energy as the sheet of water passes over the floating pipes. It also dissipates energy by wave breaking over the upper surface of the breakwater in between the openings of the pipes through turbulence and eddies. Inertia of the breakwater itself opposes the orbital motion with reflection of small part of the incident wave.

2. Dimensional analysis

The dimensional analysis is carried out using Buckingham's π theorem. The variables considered under the present investigations are: W, width of the breakwater; d, depth of water; L, wavelength; H_i, incident wave height; H_t, transmitted wave height; T, wave period; F, force in moorings; ρ, mass density of seawater; γ, density of seawater; and g, acceleration due to gravity. Considering L, H_i, and ρ as repeating variables, the dimensional analysis yields the following non-dimensional π terms: H_t/H_i (transmission coefficient, K_t), W/L, H_i/L, d/W, H_i/d, and $f/\gamma W^2$ where f is the force per unit length of the breakwater model.

3. Experimental setup

3.1. Wave flume

The experiments were conducted in the regular wave flume of the Department of Applied Mechanics and Hydraulics, NITK, Surathkal, Mangalore in Karnataka state, India. A schematic sketch of the wave flume used in the present investigations is shown in Fig. 1. The flume characteristics are as follows:

- Length of the flume: 45 m
- Flume width: 0.75 m
- Depth of flume: 1.0 m
- Type of wave flume: two dimensional
- Type of wave generator: hinged flap type
- Type of waves generated: monochromatic type
- Type of wave absorber: rubble mound spending beach

The wave flume is provided with glass panels on one side to facilitate observations and photography. The generating chamber is 6.3 m long and gradual transition is ensured between the normal flume bed level and that of generating chamber by means of a ramp. The wave filter consists of a series of vertical asbestos cement sheets spaced about 100 mm apart and kept parallel to the length of the flume. The purpose of the wave filter is to dampen the disturbance caused by successive reflections and to smoothen the generated waves. Granite stones forming a slope, act as wave absorber behind the wave generator flap in the generating chamber. The flume is provided with iron railings on the top of the sidewalls to enable the movement of a trolley. A small wire cage with coir (coir is made from coconut fiber) stuffed in it, is lowered into the flume after every run, to induce quick tranquility conditions in the flume. The wire cage is lowered by means of a roof top pulley and a long rope attached to the cage, as shown schematically (not to scale) in Fig. 1. The various wave specific and structure specific parameters considered in the present investigations are presented in Table 1.

3.2. Instrumentation and data acquisition

Linear capacitance type wave probes, along with amplification units were used to acquire incident wave height as well as transmitted wave height information. Calibrated load cells, each of 100 kg capacity with digital signal recorder were used to acquire data on the tension forces in the moorings. The calibration charts for wave probes 1 (seaside) and 2 (leeside) used in the experiments are shown in Figs. 2 and 3, respectively. Two load cells were used; one attached to the seaward side mooring and other attached to the leeward side mooring. The calibration chart for load cells 1 (seaside) and 2 (leeside) is shown in Fig. 4. The forces in both the mooring lines were recorded. The waves were generated in bursts of 5 waves to avoid

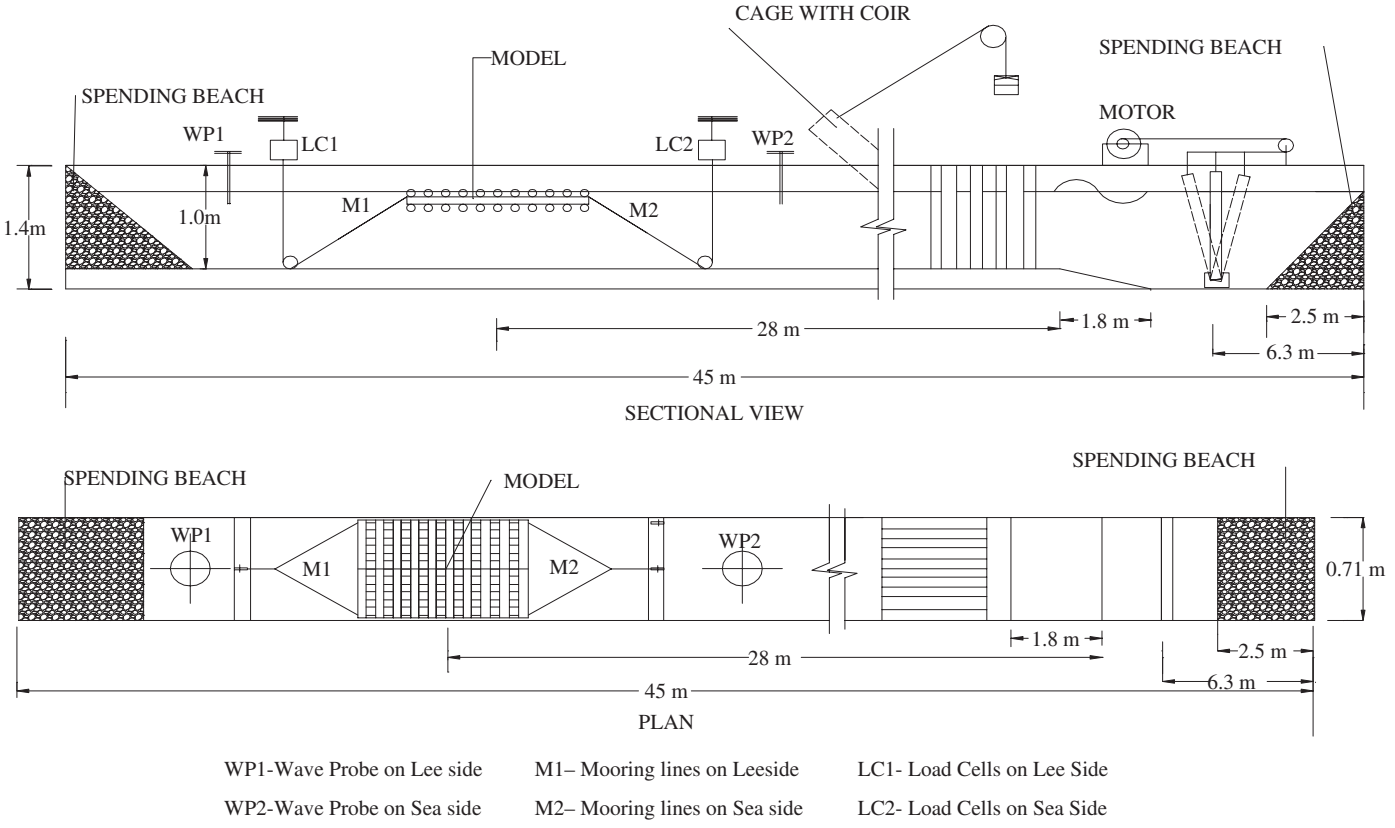

Fig. 1. Regular wave flume setup for the present investigations. WP1—wave probe on leeside, WP2—wave probe on seaside, M1—mooring lines on leeside, M2—mooring lines on seaside, LC1—load cells on leeside, LC2—load cells on seaside.

Table 1
Details of the wave-specific and structure-specific-parameters considered in the present study

Wave-specific parameters	Experimental range
Incident wave height, H_i (mm)	30, 60, 90, 120, 150, 180
Wave period, T (s)	1.2, 1.4, 1.6, 1.8, 2.0, 2.2
Depth of water, d (mm)	400, 450, 500
Structure-specific parameters	400, 450, 500
Diameter of pipes, D	32 mm
Ratio of spacing to diameter of pipes, S/D	2 and 4
Relative breakwater width, W/L	0.4 to 2.65
Number of layers, n	3

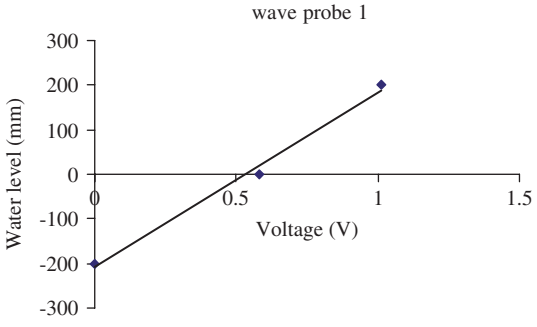

Fig. 2. Calibration chart for wave probe 1 (seaside).

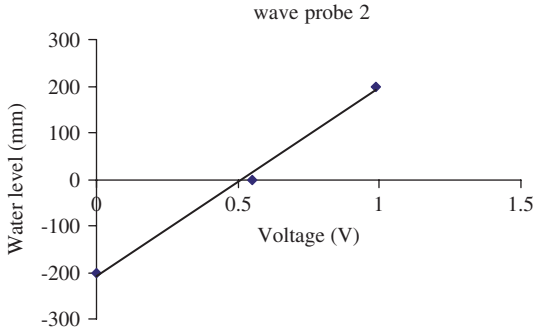

Fig. 3. Calibration chart for wave probe 2 (leeside).

wave distortion due to reflection and re-reflection in the flume. After each burst, wave generation was stopped till tranquility was achieved in the flume. Thereafter, next burst was generated. The mooring force for each burst was recorded as the maximum of values recorded for that burst. Six such trials were conducted and the average of the six values was computed, both for seaward and leeward mooring lines.

4. Breakwater model

A pictorial representation of the breakwater model in plan and section is shown in Fig. 5. The model consists of PVC pipes of 32 mm diameter. The pipes are placed parallel to each other with spacing S between them in each

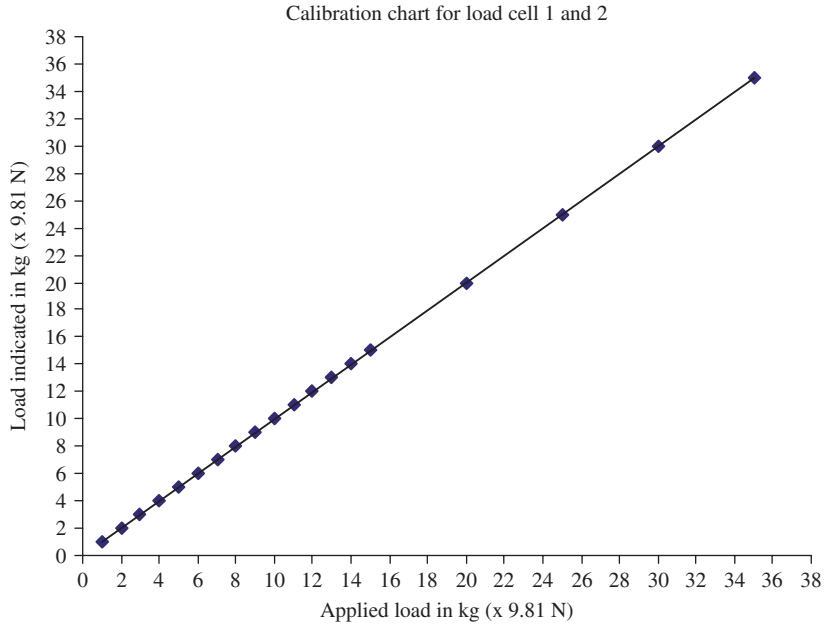

Fig. 4. Calibration chart for load cell 1 and load cell 2.

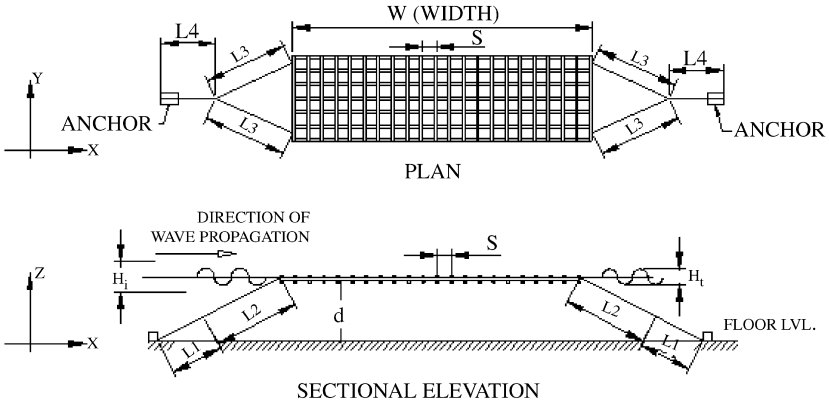

d in mm	L1 in mm	L2 in mm	L3 in mm	L4 in mm
500	558	623	604	575
450	558	623	620	557
400	558	623	635	540

Fig. 5. Floating pipe breakwater model setup used in present work.

layer, and the adjacent layers are oriented at right angles to each other so as to form an interlacing of pipes. Longitudinal pipes are placed along the direction of propagation of waves and transverse pipes are placed and tied perpendicular to longitudinal pipes. The pipes are ballasted with water till the top surface of breakwater coincides with the water surface. The length of the longitudinal pipes defines the width W of the floating breakwater. The mooring cables used were inclined as shown in Fig. 5 with a length of 1180 mm both on the seaward and leeward side. It is reasoned that with appropriate number of pipe layers n, spacing of pipes S, and relative breakwater width W/L, it is possible to achieve a considerable and effective attenuation of incident waves.

5. Experiments

In the present work, regular waves of different periods and heights as mentioned in Table 1 were generated for W/L ratios of 0.4–2.65 with model consisting of three layers (two transverse and one longitudinal) of pipes. Based on the W/L ratios used, the range of breakwater model widths used were from 0.77 to 4.91 m. The model was placed in the flume at a distance of 28 m from the flap of

the wave maker. Either ends of the breakwater model were tied with steel cables of 12 numbers of 0.025 mm diameter mild steel strands as moorings. One end of the cable was tied to the breakwater, while, other end was taken through a frictionless pulley (pulley was fixed to the bottom of the flume) and connected to the load cell, which was fixed to the frame (refer Fig. 1).

The model was constructed to suit a wave height of 5.4 m and a maximum water depth of 15 m. A geometrically similar scale of 1:30 was adopted and hence, the range of model wave heights varied from 30 to 180 mm and range of water depths varied from 400 to 500 mm. Based on this scale ratio, the model to prototype scale factors were obtained using Froude's model law.

6. Results and discussion

To study the variation of force in moorings, a normalized mooring force $f/\gamma W^2$ was considered, where f is the force/unit length of breakwater and γ the weight density of water. The variation of normalized mooring force with relative breakwater width for different values of H_i/d has been studied. The variation of seaward side and leeward side normalized mooring forces with W/L for various ranges of H_i/d values are shown in Figs. 6–9. For the data analyzed the power variation gave the largest R-squared value as compared with linear, exponential, quadratic, and logarithmic fits.

6.1. Seaward side mooring

6.1.1. Effect of relative breakwater width on normalized mooring force

The variation of $f/\gamma W^2$ in the seaward side with W/L for different ranges of H_i/d values is shown in Fig. 6 for breakwater model with relative spacing of 2. The graphs show a decrease in $f/\gamma W^2$ with an increase in W/L up to a value of 1.3. Thereafter effect of W/L is not significant. The probable reason for this behavior is that for small W/L values, the wavelength is more than the breakwater width, leading to the presence of either the crest or the trough on the

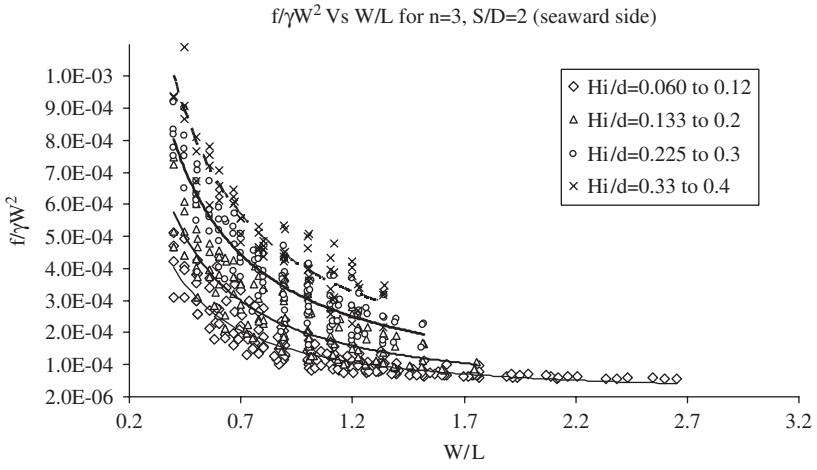

Fig. 6. Variation of $f/\gamma W^2$ (seaward) with W/L for $n = 3$ and $S/D = 2$ for a range of H_i/d values.

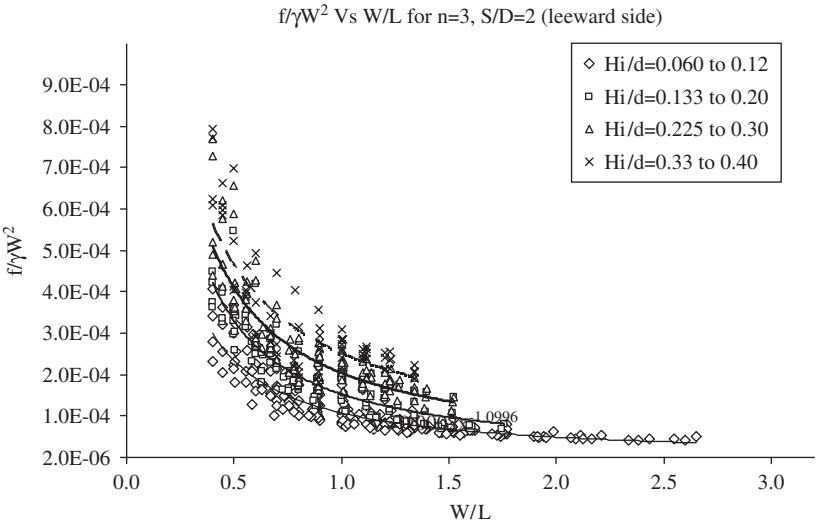

Fig. 7. Variation of $f/\gamma W^2$ (leeward) with W/L for $n = 3$ and $S/D = 2$ for a range of H_i/d values.

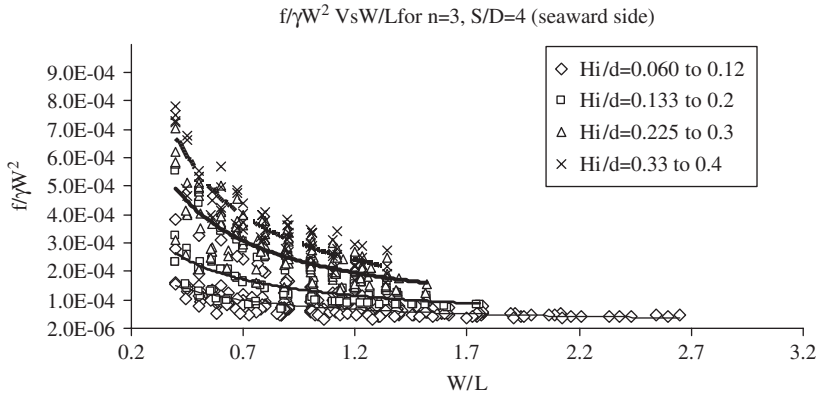

Fig. 8. Variation of $f/\gamma W^2$ (seaward) with W/L for $n = 3$ and $S/D = 4$ for a range of H_i/d values.

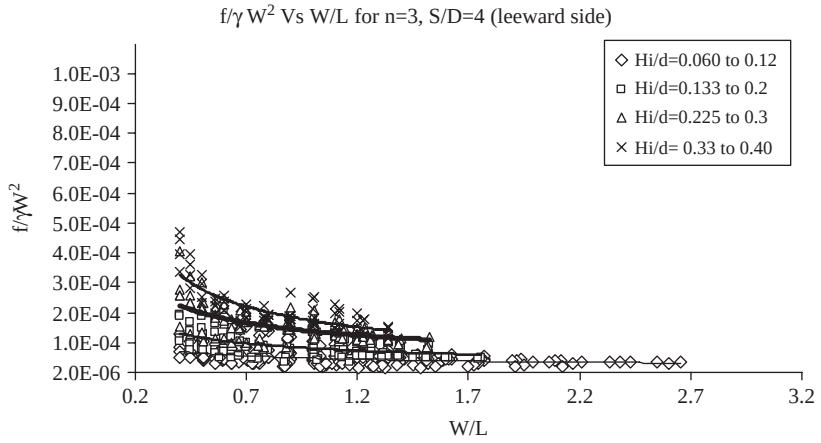

Fig. 9. Variation of $f/\gamma W^2$ (leeward) with W/L for $n = 3$ and $S/D = 4$ for a range of H_i/d values.

breakwater model. This results in larger mooring forces, but rapidly decreases for higher values of W/L (in the range of 0–1.3). As W/L increases further, the wavelength is shorter or equal to breakwater width, leading to the presence of both crest and trough and a gradual decrease in forces in the moorings. Further, it was observed that for H_i/d value of 0.06, maximum $f/\gamma W^2$ was 4.7×10^{-4} and for H_i/d value of 0.40, maximum $f/\gamma W^2$ was 1.2×10^{-3}. This indicates that as H_i/d increases, force in the seaward side moorings also increases, and is reflected in the graphs in Fig. 6. The graphs also indicate that as the depth of water decreases, $f/\gamma W^2$ increases for given value of W/L, reflecting the fact that for small depths, energy distribution is nearly uniform along the depth; however, depth of submergence of breakwater model being a constant, the percentage of energy intercepted by the breakwater was more, indicating larger forces. The normalized force for H_i/d value of 0.40 was 2.55 times that for H_i/d value of 0.06. This clearly emphasizes the influence of H_i/d on $f/\gamma W^2$.

The variation of normalized force with relative breakwater width for relative spacing of 4 is shown in Fig. 7. The behavior is similar to that observed for breakwater with relative spacing of 2. For H_i/d value of 0.06, maximum $f/\gamma W^2$ observed was 2.8×10^{-4} and for H_i/d value of 0.40, maximum $f/\gamma W^2$ was 7.5×10^{-4}. The normalized force for H_i/d value of 0.40 is 2.67 times that for H_i/d value of 0.06. For relative spacing of 2, forces in the moorings were higher than that compared with relative width of 4. This implies that breakwater with relative spacing of 2 reflects more incident wave energy due to its low porosity, compared to relative spacing of 4. A multivariate nonlinear regression analysis was carried out for mooring force data for the seaside, and the following regression models were obtained, for relative spacing of 2 (Eq. (1)) and 4 (Eq. (2)):

$$\frac{f_s}{\gamma W^2} = 0.000347 \times 0.3348^{W/L} \times 42.58^{H_i/d}, \quad (1)$$

$$\frac{f_s}{\gamma W^2} = 0.000124 \times 0.479^{W/L} \times 147.81^{H_i/d}, \quad (2)$$

where f_s is the seaward side force per unit length of breakwater.

6.2. Leeward side mooring

6.2.1. Effect of wave steepness on normalized mooring force

The variation of normalized force in the leeward side with W/L for different ranges of H_i/d values are shown in Figs. 7 and 9 for models with relative spacing of 2 and 4,

respectively. The influence of W/L on the normalized force was not significant for the range of H_i/d values between 0.06 and 0.20 and also for $H_i/d = 0.30$. However, the general trend that may be noticed is a decrease in $f/\gamma W^2$ with an increase in W/L. Further, it was observed that for H_i/d value of 0.06, maximum $f/\gamma W^2$ was 8.6×10^{-5} and for H_i/d value of 0.40, maximum $f/\gamma W^2$ was 4.5×10^{-4}. The $f/\gamma W^2$ for H_i/d value of 0.40 is 5.23 times greater than that for H_i/d value of 0.06. The maximum $f/\gamma W^2$ on seaward side was 3.29 times greater than that for leeward side, for H_i/d value of 0.06 and relative spacing of 4. Similarly, normalized force on seaward side mooring was 1.66 times greater than that for leeward side mooring for H_i/d value of 0.40 and relative spacing of 4.

The $f/\gamma W^2$ on seaward side of breakwater with relative spacing of 2 was 1.67 times and 1.6 times greater than that with relative spacing of 4, for H_i/d values of 0.06 and 0.40, respectively. The normalized force on leeward side mooring of breakwater with relative spacing of 2 was 4 times and 1.71 times greater than that for relative spacing of 4, for H_i/d value of 0.06 and 0.40, respectively. Maximum force in seaward side mooring for S/D of 2 was 80.44 N and that with relative spacing of 4 was 60.82 N and this corresponds to values of H_i/L of 0.0397, H_i/d of 0.36, and W/L of 1.2. Similarly, the maximum force in leeward side mooring with relative spacing of 2 was 50.03 N and that with relative spacing of 4 was 40.71 N and this too corresponded to values of H_i/L of 0.0397, H_i/d of 0.36, and W/L of 1.2. Multivariate nonlinear regression analysis was carried out for the data on mooring forces for leeward side too, and the following regression models were obtained, for relative spacing of 2 (Eq. (3)) and 4 (Eq. (4)):

$$\frac{f_l}{\gamma W^2} = 0.000276 \times 0.361^{W/L} \times 17.53^{H_i/d}, \tag{3}$$

$$\frac{f_l}{\gamma W^2} = 0.0000575 \times 0.6347^{W/L} \times 135.66^{H_i/d}, \tag{4}$$

where f_l is the leeward side force per unit length of breakwater.

The scope of this paper is study of mooring forces on two breakwater models with different relative spacings. However, a brief discussion on its wave attenuation characteristics is worth mentioning. The maximum wave attenuation by breakwater model with relative spacing of 4 was 55.7% (Hegde et al., 2006) and that by model with relative spacing of 2 was 51.7%. This indicates that the model with relative spacing of 4 attenuates more incident energy by dissipation as the wave passes over the breakwater. Fig. 10 shows the variation of transmission coefficient K_t with W/L for a range of values of H_i/d from 0.060 to 0.12, for relative spacing of 2 and 4 with three layers of pipe. The graphs clearly indicate that the breakwater model with relative spacing of 4 has better attenuation performance than that with relative spacing of 2.

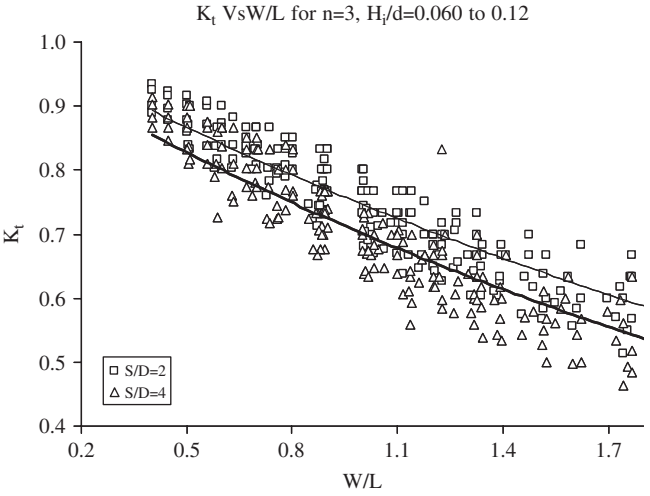

Fig. 10. Variation of K_t with W/L for $n = 3$ and $H_i/d = 0.060$–0.12.

7. Conclusions

Based on the present investigations and results obtained, the following conclusions are drawn:

The normalized force increases with an increase in H_i/L, and decreases with an increase in W/L. The normalized force shows an increasing trend beyond a W/L value of 1.3. The forces in the moorings are more in breakwater with relative spacing of 2 than that with relative spacing of 4. Influence of H_i/d is significant on the normalized force. The maximum measured force on seaward side mooring of the model with relative spacing of 2 was 80.44 N and that with relative spacing of 4 was 60.82 N, corresponding to values of H_i/L of 0.0397, H_i/d of 0.36, and W/L of 1.2. This indicates that mooring forces with relative spacing of 2 is more than that with relative spacing of 4. The forces in both the moorings (seaward side and leeward side) were maximum corresponding to values of H_i/L of 0.0397, H_i/d of 0.36, and W/L of 1.2. The seaward side mooring forces were found to be always higher than the corresponding leeward side mooring forces. Maximum wave attenuation by breakwater model with relative spacing of 2 was 51.7% and that by breakwater model with relative spacing of 4 was 55.7%.

Acknowledgment

The authors would like to express their sincere thanks to the Director, National Institute of Technology Karnataka, Surathkal, Mangalore, India for providing all the necessary infrastructural facilities required for the present study.

References

Arunachalam, V.M., Raman, H., 1980. Discussion of design criteria for floating tire breakwater. Journal of Waterway, Port, Coastal, and Ocean Engineering, ASCE 106 (2), 296–298.

Bishop, T.C., 1982. Floating tire breakwater design comparison. Journal of Waterway, Port, Coastal, and Ocean Engineering, ASCE 108 (3), 421–426.

Brebner, A., Ofuya, A.O., 1968. Floating breakwaters. In: Proceedings of the 11th Coastal Engineering Conference, London, England, pp. 1055–1094.

Chen, K., Wiegel, R.L., 1970. Floating breakwaters for reservoir marinas. In: Proceedings of the 12th Coastal Engineering Conference, Washington, DC, vol. III, pp. 1647–1666.

Harms, V.W., 1979. Design criteria for floating tire breakwater. Journal of Waterway, Port, Coastal, and Ocean Engineering, ASCE 106 (2), 149–170.

Harris, A.J., Webber, N.B., 1968. A floating breakwater. In: Proceedings of the 11th Coastal Engineering Conference, London, England, pp. 1049–1054.

Hegde, A.V., Kamath, K., Deepak, J.C., 2006. Transmission characteristics of horizontal interlaced moored floating pipe breakwaters with three layers and relative spacing of four—effect of wave steepness, relative width. In: Proceedings of HYDRO 2006, National Conference on Hydraulics and Water Resources, ISH, Pune, India, pp. 611–620.

Hegde, A.V., Kamath, K., Magadum, A.S., 2007. Performance characteristics of horizontal interlaced multilayer moored floating pipe breakwater. Journal of Waterway, Port, Coastal, and Ocean Engineering, ASCE 133 (4), 275–286.

Isaacson, M., Wu, S.R., 1995. A numerical study of moored vessel response to beam waves. In: Proceedings of the Fifth International Offshore and Polar Engineering Conference, Netherlands, vol. 3, pp. 499–506.

Mani, J.S., 1991. Design of Y-frame floating breakwater. Journal of Waterway, Port, Coastal, and Ocean Engineering, ASCE 117 (2), 105–119.

Miller, R.W., Christensen, D.R., 1984. Rigid body motion of a floating breakwater. In: Proceedings of the Coastal Engineering Conference, pp. 2663–2679 (Chapter 179).

Murali, K., Mani, J.S., 1997. Performance of cage floating breakwater. Journal of Waterway, Port, Coastal, and Ocean Engineering, ASCE 123 (4), 172–179.

Sannasiraj, S.A., Sundar, V., Sundaravadivelu, R., 1998. Mooring forces and motion response of pontoon-type floating breakwaters. Ocean Engineering 25 (1), 27–48.

Sundar, V., Sundaravadivelu, R., Purushotham, S., 2003. Hydrodynamic characteristics of moored floating pipe breakwater in random waves, Proceedings of the Institution of Mechanical Engineers. Journal of Engineering Maritime Environment 217M, 95–108.

Yamamoto, T., 1981. Moored floating breakwater response to regular and irregular waves. Applied Ocean Research 3, 114–123.

Yamamoto, T., Yoshida, A., Ijima, T., 1980. Dynamics of elastically moored floating objects. Applied Ocean Research 2, 85–92.